

ICES CM 2004/M:01

Theme Session M. Regime Shifts in the North Atlantic Ocean: Coherent or Chaotic?

Temporal linkages between the Faroe-Shetland time series and the Kola section time series

Harald Yndestad, William R Turrell, Vladimir Ozhigin

Abstract

The Faroe-Shetland time series and the Kola time series cover a time period of more than hundred years and represent two of the longest oceanographic time series in the world. The relationship between these important time series is examined in this paper, which presents for the first time comparisons between the annual mean sea level and the temperature and salinity of Atlantic Water in the Faroe-Shetland Channel and the Kola section in the Barents Sea. The investigation is based on a wavelet spectrum analysis used to identify the dominant cycle periods and cycle phases in all time series. The identified cycles are compared to dominant cycles in sea level time series from Aberdeen and Hammerfest.

The investigation has identified a correlation better than $R=0.8$ between dominant temperature cycles and the 18.6 year lunar nodal tide in most time series. The paper presents the correlations to the lunar nodal tide, the phase relationships between the dominant cycles and the signal to noise ratio between the dominant cycles and other unknown sources. The identified 18 year cycles seem to have a temporary stationary cycle time and a time variant phase. The dominant 18 year temperature and salinity time series in the Faroe-Shetland Channel and the Kola section had a phase-reversal that started in about 1920-25. A cycle phase-reversal may be explained by an amplitude modulation between the 18 year cycle and a more low frequent cycle.

Keywords: 18.6 year lunar cycle, decadal variability, Atlantic water, NE Atlantic, Barents Sea, wavelet analysis, climate prediction

Harald Yndestad: Aalesund University College, N-6025 Aalesund, Norway.

Tel: +47 70 16 12 00; fax: +47 70 16 13 00; e-mail: Harald.Yndestad@hials.no

William R Turrell: FRS Marine Laboratory Aberdeen, PO Box 101, Victoria Road, Aberdeen, AB11 9DB, Scotland. Tel :+44 (0)1224 876544. Fax :+44 (0)1224 295511, E-mail :turrellb@marlab.ac.uk

Vladimir Ozhigin: Polar Research Institute of Marine Fisheries and Oceanography (PINRO), 6 Knipovich St., Mermansk, 183763 Russia. Tel: +007 8152 47 32 80; fax: +007 8152 47 33 31; e-mail: ozhigin@pinro.ru.

Introduction

The Faroe-Shetland Channel time series

The Faroe-Shetland Channel is the deep water channel separating the Faroese plateau from the Scottish continental shelf. The northern entrance from the Norwegian Sea is approximately 1500 m - 2000 m deep. Connections to the Atlantic lie to the southwest through the Faroe Bank Channel, with maximum depths of 850 m, and across the Wyville-Thomson Ridge, with a sill depth of approximately 450 m. Two standard hydrographic sections across the Channel have been surveyed by the Fisheries Research Services Marine Laboratory since the start of the 20th century. These lines run approximately from Fair Isle to Munken (Faroe) and from Nolso (Faroe) to Muckle Flugga (Shetland). They were first surveyed by Dr H N Dickson, contracted to the Fishery Board for Scotland, on board the fishery protection vessel HMS Jackal. He performed the first hydrographic station of the Nolso - Flugga section on 4 August 1893. He went on to perform water bottle casts at four stations of the present day Nolso - Flugga section and at three stations of the Fair Isle - Munken section. Dickson resurveyed the same sections in 1896. Although fewer stations were performed during that survey, deeper casts were achieved, reaching >1,000 m. Regular sampling at the full set of Nolso - Flugga and Fair Isle - Munken stations commenced in 1903, and has been performed approximately three times each year since then, except for the war years and for a five year period in the early 1980s.

A database of all available data collected along the two standard sections was constructed using data which existed in digital form from 1960 onwards, and using data from original manuscripts prior to that date. After the data was extracted, it was interpolated onto standard pressure levels. These procedures are more fully described in Turrell et al. (1999). In addition to data collected by the FRS Marine Laboratory, data from other sources, including Faroese, Norwegian, Swedish, Danish, English and Russian institutes, was obtained from ICES and entered into the database. Time-series derived from the observations along the two sections have been employed in numerous previous publications (see Turrell et al. 1999).

In the previous studies time-series were constructed subjectively using manual methods from section plots and σ_t diagrams. Since the creation of the database, objective semi-automatic generation of time-series have been used in order to determine the characteristics of the different water masses observed along the sections. Two principal "types" of surface Atlantic water are always observed across the sections; a warmer and more saline type referred to as North Atlantic Water (NAW), and a fresher, cooler type referred to as Modified North Atlantic Water (MNAW). NAW lies in the Slope Current which flows northwards along the European shelf edge. MNAW arrives at the standard sections after circulating around to the north of Faroe. The methods used to determine the properties of these water masses are described below.

The Kola section and Kola section time series

The International Conference on Exploration of the Sea, held in 1899 in Stockholm, recommended that observations along a standard section running north from the Kola fjord (along 33°30' E) and into the Barents Sea should be carried out. The section runs across the Coastal Water having warm temperatures and low salinity (St. 1-3; 69°30' -70°30'N, 33°30'E). The northern stations (8 through 10; 73°00' -74°00'N, 33°30'E) where highest salinities are measured are considered as Atlantic Water. The stations ranging from 3 to 7 (70°30' -72°30'N, 33°30'E) are associated with the Murman Current. To study seasonal and interannual variability of temperature and salinity, the data are averaged vertically over 4 depth intervals (0-50, 0-200, 50-200 and 150-200 m) and horizontally over 3 parts of the Section. Temperature averaged over the upper 200 m and over stations 3 through 7 (70°30' -72°30'N, 33°30'E) produces a well-known and widely used time-series.

The Murman Fishery Research Expedition led by N. Knipovich occupied the section for the first time in 1900. The Expedition was completed in 1906. During that period the section was occupied 1-6 times a year. Then it was not occupied until 1921. In 1920-1930 the section was occupied from 1 (1924) to 10 (1937) times a year. The next gap in observations is related to World War Two. The Section has been occupied most frequently since the middle of the 1950s with often more than 12 surveys each year. In 1970-1980 the annual number of occupations exceeded 15. A considerable decrease in occupation of the section occurred in the early 1990s. In the 1990s and at present PINRO took measurements along the section about 10 times a year. By the present time (2004) the Kola Section had been surveyed more than 950 times.

The gaps in the time series were filled by Bochkov (1982) by means of calculations by multiple regression models. To calculate quarterly and yearly temperatures for 1900-1920 and 1941-1944, air temperature at stations Kola and Polyarny, the number of deep low pressure cells (cyclones) over the Norwegian and Greenland Seas and the ratio of the number of deep cyclones over the Barents Sea to the number of deep cyclones over the Norwegian and Greenland Seas, were used as the independent variables in the regression models. Owing to high correlation between monthly and quarterly time series, monthly temperature values for 1941-1944 were calculated by simple regression models, quarterly temperature time series were used as independent variables. Thus, quarterly and annual temperature values are available from 1900 to 2003. The monthly time series begins in 1921.

The time series of salinity begins in 1951 owing to some uncertainties in the quality of the data collected during the first half of the 20th century. The Kola section time series of temperature and salinity were published in the following publications: Bochkov Yu.A. 1982. Water temperature in the 0-200 m layer in the Kola Meridian Section in the Barents Sea, 1900-1981. *Sb. Nauch. Trud. PINRO*. 46: 113-122 (in Russian). Quarterly and yearly temperature values from 1900-1920; Monthly temperature values from 1941-1981. Tereshchenko V.V. 1997. Seasonal and year-to-year variation in temperature and salinity of the main currents along the Kola section in the Barents Sea. *Murmansk: PINRO Publ.* 71 pp. (in Russian). Monthly and yearly temperature and salinity values from 1941-1981.

The Kola section temperature time series (St. 37, 0-200 m) can be used to assess seasonal and interannual variability of hydrographic conditions in the southern Barents Sea. There is a significant correlation ($r=0.7-0.9$) between this time series and those for stations 1-3 and 8-10 of the Kola transect (Tereshchenko, 1997). There is also a significant correlation ($r=0.7-0.9$) between temperature time series from the Kola section and other standard sections in the southern Barents Sea (North Cape - Bear Island section at the Barents Sea opening; Bear Island - East section (along 74°30'N) in the western Barents Sea; Cape Kanin -North section (along 43°15'E) in the eastern Barents Sea).

The general opinion is that the Kola section time series can serve as a reliable indicator of climate variability in the whole southern Barents Sea (coastal and Atlantic water domain). Besides, there is a significant correlation ($r=-0.56$ - monthly data; $r=-0.65$ - yearly data) between time series of temperature in the Kola section and ice coverage (% of the total Barents Sea area). However, this is not true for the salinity time series from stations 3-7. Correlation between temperature and salinity time-series from stations 3-7 is close to zero. This is probably due to the fact that there is a well pronounced haline frontal zone (between 71 and 72 deg. N, st. 4 and 6) separating Atlantic water (warm temperature, high salinity), to the north, and slightly warmer and considerably fresher Coastal water, to the south. Therefore, variability of salinity averaged for st. 3-7 may very much depend on variations of the haline front position, and this is yet to be studied.

Stations 3-7 are usually associated with the Murman Current, which is the continuation of the North Cape Current entering the Barents Sea through its western boundary. The Murman Current is related

to the haline/density frontal zone. According to calculations by a numerical model (Trofimov, 2000) the core of the current is located at about $72^{\circ}00'N$.

The problem of time series analysis

A time series from nature may have time variant stochastic properties. These properties introduce a reference problem when a data series is analyzed by traditional statistical or spectrum analysis methods. To overcome this problem the time series first are filtered by a wavelet transformation. A wavelet transform has the ability to identify both period and phase cycles in time series. The identification of the phase cycle opens a possibility to compare events between different time series. This investigation compares the period and phase cycles to identified known geophysical cycles and the phase relation between the dominant cycles is examined. The result shows that most of the long-term fluctuations are associated with harmonics from the 18.6-year lunar nodal tide.

Materials and methods

The Faroe-Shetland Channel data series

It has been found that the best definition of the properties of North Atlantic Water, found within the core of the Slope Current on the Scottish side of the Faroe-Shetland Channel, is the temperature and salinity at the standard depth which exhibits the maximum salinity within an individual survey of the first two stations, on both standard sections, on the Scottish side of the Channel.

As the standard section surveys during the past have been performed at quite different times of the year, in order to remove the effect of the seasonal cycle in the surface waters, and hence allow all data to be used, the monthly mean temperature and salinity derived over the period 1960-1995 for each individual station and at each standard depth have been removed prior to smoothing the data using a 2-year centered running mean. Hence the data are expressed as anomalies. The data series covers 1893...2002 and has no values from 1895...1902, 1915...1922, 1930...1933, 1941...1946. In these periods the data are interpolated.

For Modified North Atlantic Water, located on the Faroese side of the Channel, the definition used is the temperature and salinity at the standard depth which exhibits the maximum salinity within an individual survey of the first two stations, on both standard sections, on the Faroese side of the Channel. Again the seasonal cycle has been removed prior to smoothing using a 2-year running mean. Hence the data are presented as anomalies. The data series covers 1893...2002 and has no values from 1895...1902, 1915...1922, 1930...1933, 1941...1946. In these periods the data are interpolated.

The Kola data series

The data used here are monthly temperature values from the upper 200 m in the Kola section along the $33^{\circ}30'E$ medial from $70^{\circ}30'N$ to $72^{\circ}30'N$ in the Barents Sea (Bochkov, 1982; Tereshchenko, 1997)). The temperature data series contains quarterly and annual values from the period 1900-2003 and monthly values from 1921, some of which are measured and some of which are calculated. Salinity time series (monthly and annual values) is available only from the period 1951-2003. This paper analyzes the annual mean temperature and salinity.

The Aberdeen tide data series

The time series of sea level at Aberdeen is provided by the Proudman Oceanographic Laboratory, UK. The data series has an annual mean and covers the period 1931 to 2002.

The Hammerfest tide data series

The time series of sea level at Hammerfest is provided by Statens Kartverk in Norway. The time series has the mean monthly values from 1957 to 2002. In this analysis the data series is reduced to the annual mean in the same period.

Cycle identification

The Fourier spectrum $X(j\omega)$ of a time series $x(t)$ may be represented by the model:

$$X(j\omega) = U(j\omega) + V(j\omega) \quad (1)$$

where $U(j\omega)$ represents a known spectrum and $V(j\omega)$ represents a non-correlated red spectrum from an unknown source. One of the main problems encountered in this analysis is identifying a known spectrum $U(j\omega)$ in the total spectrum $X(j\omega)$. A possible stationary cycles $U(j\omega)$ may have a time-variant amplitude and phase. A time variant phase makes it difficult to identify stationary cycles with straightforward statistical methods. A second problem is that it can be difficult to identify low frequency cycles and to separate the high frequency cycles from noise in these short time series. Wavelet transformation is an appropriate method to analyze time-variant data series. A continuous wavelet spectrum is computed by the wavelet transformation:

$$W(a,b) = \frac{1}{\sqrt{a}} \int_R x(t) \Psi\left(\frac{t-b}{a}\right) dt \quad (2)$$

where $x(t)$ is the analyzed time series, $\Psi(\cdot)$ is a wavelet impulse function, $W(a,b)$ is the computed wavelet cycles, b is a translation in time and a is a time scaling parameter in the wavelet filter function. The computed wavelets $W(a,b)$ represent a set of filtered time series from the time series $x(t)$ and the impulse functions $\Psi(\cdot)$. In the following analysis, a Coiflet3 wavelet transform was chosen from many trials on tested data (Matlab, 1997; Daubechies, 1992). The wavelet transformation represents a linear phase filter that is able to separate additive cycles in a time series. In this analysis the time series is scaled by $x(t) = (\text{mean}(x(t)) - \text{var}(x(t))) / \text{var}(x(t))$ to reduce transformation side effects.

A discrete time series $x(nT)$ may be represented by a sum of dominant wavelet cycles

$$x(nT) = \sum_k W(k, nT) + v(nT) = W(nT) + v(nT) \quad (3)$$

where k is a cycle period, T is the sampling period, n is the sample number, $W(k, nT)$ represents a dominant wavelet cycle, $W(nT)$ represents the sum of wavelet cycles, and $v(nT)$ is a disturbance from an unknown source. A wavelet cycle $W(k, nT)$ represents a moving correlation to an impulse period k . A dominant cycle period thus represents the best correlation to a cycle period k . If the dominant cycle is a stationary cycle, the time series may be represented by

$$x(nT) = \sum_k U(k, nT) + v(nT) = \sum_k u(k, nT) \sin(\omega_0 nT + \mathbf{j}(nT)) + v(nT) \quad (4)$$

where $U(k, nT)$ represents a known stationary cycle and $v(nT)$ is a disturbance from an unknown source. The time series has the same cycles and disturbance if $U(k, nT) = W(k, nT)$. The known spectrum $U(j\omega)$ is identified in the wavelet spectrum by computing the cross-correlation quotient:

$$R(k) = E[U(k, nT)W(k, nT)] \quad (5)$$

where $U(k, nT)$ is the cycle k in the known spectrum $U(j\omega)$ and $W(k, nT)$ is the cycle k in the computed wavelet spectrum. The wavelet cycle time k is tested by computing the correlation coefficient $R(k)$

between the dominant wavelet cycle $W(k,nT)$ and a potential known stationary cycle $u(j^?_k)$. The correlation value of quality is computed by $Q(k)=R(k)*\text{sqrt}[(N-2)/(1-R(k)*R(k))]$ where N is the number of samples in the time series.

The cycle amplitude dominance is identified by the signal-to-noise ratio. The signal-to-noise ratio between the dominant wavelet cycles $W(nT)=K_1W(k1,nT)+K_2W(k2,nT)+K_3W(k3,nT)$ and the unknown source $v(nT)$ is computed by:

$$S / N = \text{var}(W(nT)) / \text{var}(v(nT)) \quad (5)$$

where $v(nT) = (x(nT)-W(nT))$ represents the estimated disturbance from an unknown source. A single dominant cycle have a set of maximum values $W(k1,nT)_{\text{max}} = \{W1, W2, \dots Wn\}$.

Results

This investigation is based on a wavelet analysis of time series of sea level, Atlantic water temperature and Atlantic water salinity at two locations in the Nordic Seas; the Faroe-Shetland Channel and at the Kola section in the Barents Sea.

The analysis of the Faroe-Shetland Channel and Kola Section time series are shown in figures 1 to 8. The dominant cycles in the time series are correlated to the lunar nodal spectrum in order to identify any possible relation. The 18.6 year lunar nodal cycle has a maximum in November 1987 when the cycle phase $\phi_{\text{nut}}(18)=0.90\pi$ (rad) (Pugh, 1969). A summary of the investigation is presented in Table 1.

MNAW Temperature

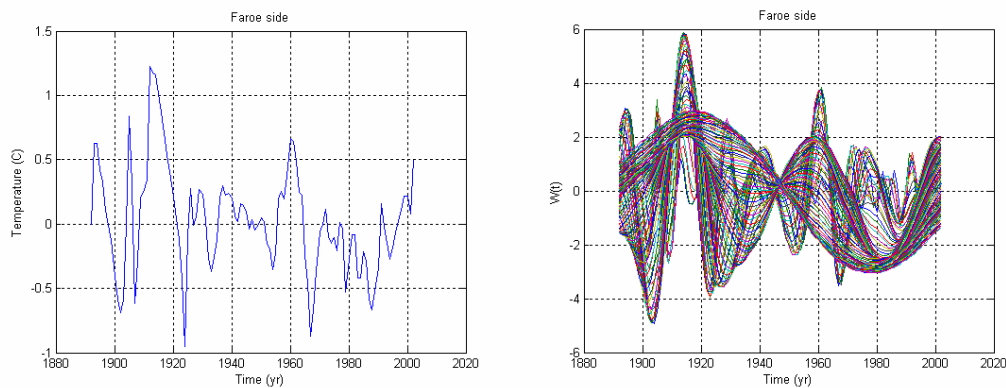


Figure 1 Time series of Modified North Atlantic Water (MNAW) temperature on the Faroe side of the Faroe-Shetland Channel and the computed wavelet spectrum.

Figure 1 shows the analyzed time series of the Modified North Atlantic Water (MNAW) temperature on the Faroe side of the Faroe-Shetland Channel from 1893 to 2002. Also shown are the computed total wavelet spectrum $W_{\text{FarTemp}}(4:80,nT)$. The wavelet spectrum $W_{\text{FarTemp}}(4:80,nT)$ has dominant wavelet cycles of about 6, 18 and 55 years. These are the same periods as the lunar nodal spectrum of $18.6/3=6.2$, 18.6 and $18.6*3=55.8$ years.

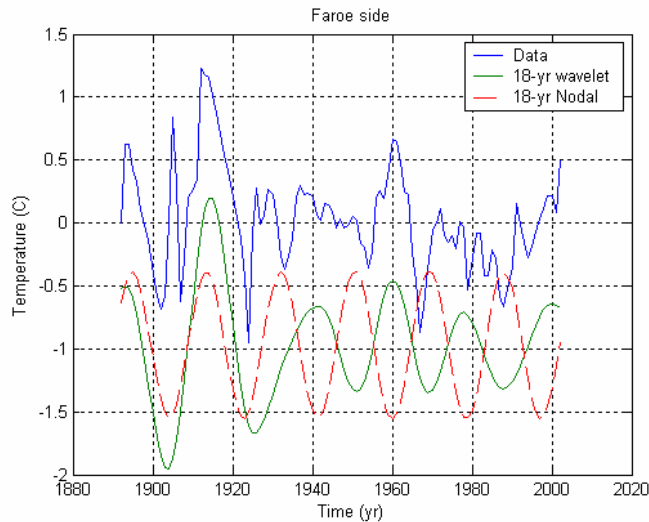


Figure 2 Modified North Atlantic Water (MNAW) temperature on the Faroe side of the Faroe-Shetland Channel, 18 year wavelet cycle and the 18.6 yr lunar nodal tide. In this presentation the cycles are scaled by -1.

Figure 2 shows the MNAW temperature data series, the identified 18 year wavelet cycle and the stationary 18.6 yr lunar nodal tide cycle. The identified 18 year wavelet cycle has maximum at about $W_{FarTemp}(18, nT)_{max} = \{1913, 1940, 1960, 1978, 2000\}$. The figure shows that the 18 year wavelet cycle follows the 18.6 yr tide from about 1893 to 1920. At around 1920 there is a phase-reversal of p (rad) and the 18 yr temperature cycle follows the inverse 18.6 year lunar nodal tide from about 1940 to 2000. The cross-correlation to the 18.6 yr lunar nodal tide is estimated to $R_{FarTemp}(18)_{max} = E[W_{FarTemp}(18, nT)U_{nod}(18, nT)] = -0.91$ in the period $n=1920\dots 2003$. A cross-correlation to the third sub-harmonic cycle $3*18.5=55$ years is estimated to $R_{FarTemp}(55)_{max} = E[W_{FarTemp}(55, nT)U_{nod}(55, nT)] = 0.8$ when $n=1893\dots 2003$. The signal to noise relation is estimated to $S/N=5.4$ when the signal is wavelets cycles of 6, 18 and 55 years.

MNAW Salinity

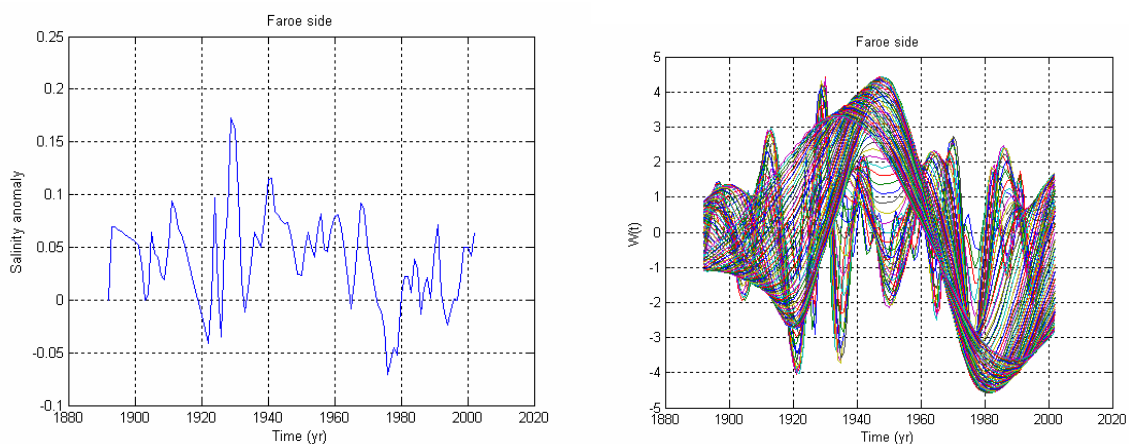


Figure 3 Time series data of Modified North Atlantic Water (MANW) salinity on the Faroe side of the Faroe-Shetland Channel and the computed wavelet spectrum.

Figure 3 shows the analyzed time series of Modified North Atlantic Water (MNAW) salinity on the Faroe side of the Faroe-Shetland Channel from 1893 to 2002, as well as the wavelet spectrum

$W_{\text{FarSal}}(4:80,nT)$ of Modified North Atlantic Water salinity. The wavelet spectrum $W_{\text{FarSal}}(4:80,nT)$ has dominant cycles of about 6, 18 and 55 years. The cycles are as the lunar nodal spectrum.

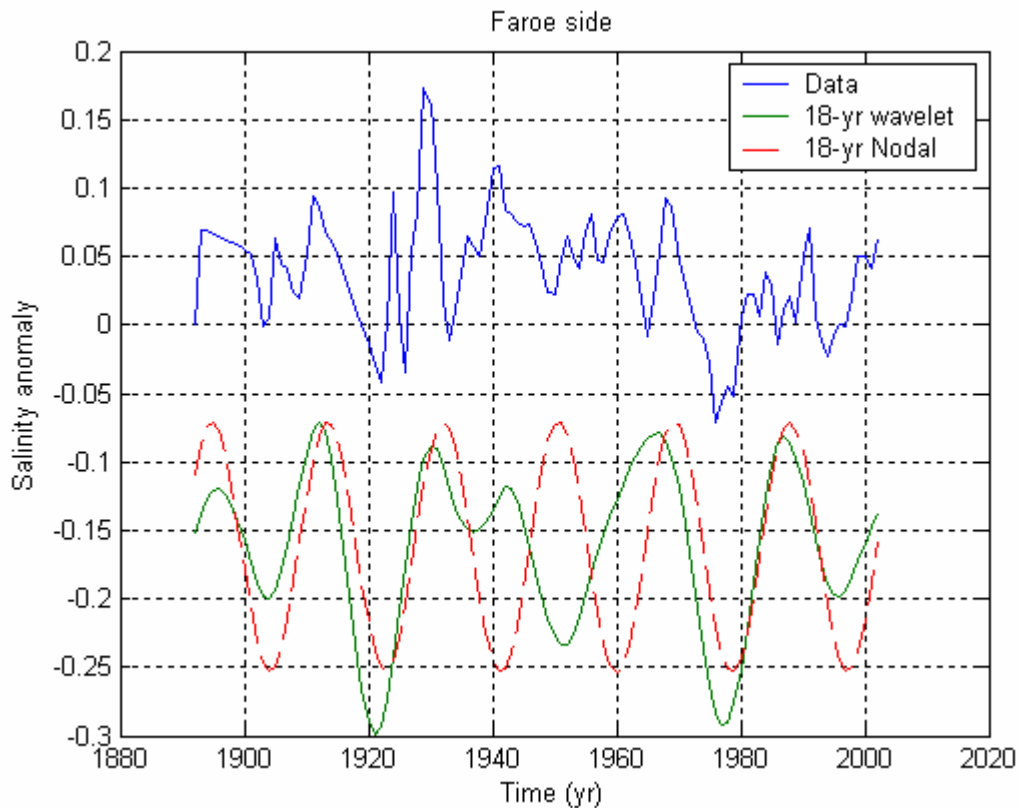


Figure 4 The Modified North Atlantic Water (MNAW) salinity on the Faroe side of the Faroe-Shetland Channel, the dominant 18 yr cycle and the stationary 18.6 yr lunar nodal tide. The cycles are scaled by -1 on this figure.

Figure 4 shows the identified dominant 18 yr salinity cycle and the stationary representation of the 18.6 yr lunar nodal tide. The 18 year cycle has a maximum at about $W_{\text{FarSal}}(18,nT)_{\text{max}}=\{1895, 1912, 1930, 1942, 1965, 1987\}$. The figure shows there is a close relation between the 18 yr cycle and the 18.6 yr lunar nodal tide in the period 1893 to 1920, a phase-reversal of π (rad) in the period 1920 to 1978 and in 1978 to 2002 there has been a new phase-reversal. The cross-correlation with the 18.6 yr lunar nodal tide is estimated to $R_{\text{FarSal}}(18)=E[W_{\text{FarSal}}(18,nT)U_{\text{noda}}(18,nT)]=0.82$ when the cycle was reversed in the period $n=1920\dots1978$. The signal to noise relation was estimated to $S/N=2.6$.

The Kola section temperature time series

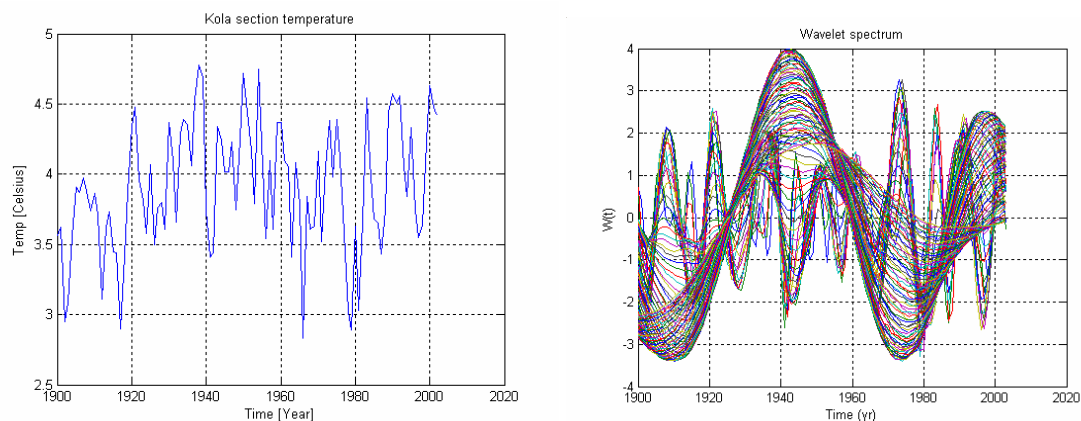


Figure 5 Time series of Kola section temperature series and the wavelet spectrum and the computed wavelet spectrum.

Figure 5 shows the Kola section time series and the computed wavelet spectrum $W_{\text{KolTmp}}(4:80, nT)$. In this wavelet set the dominant cycles are identified at about 6, 18, 55 and 74 years, and again correspond to the lunar nodal spectrum.

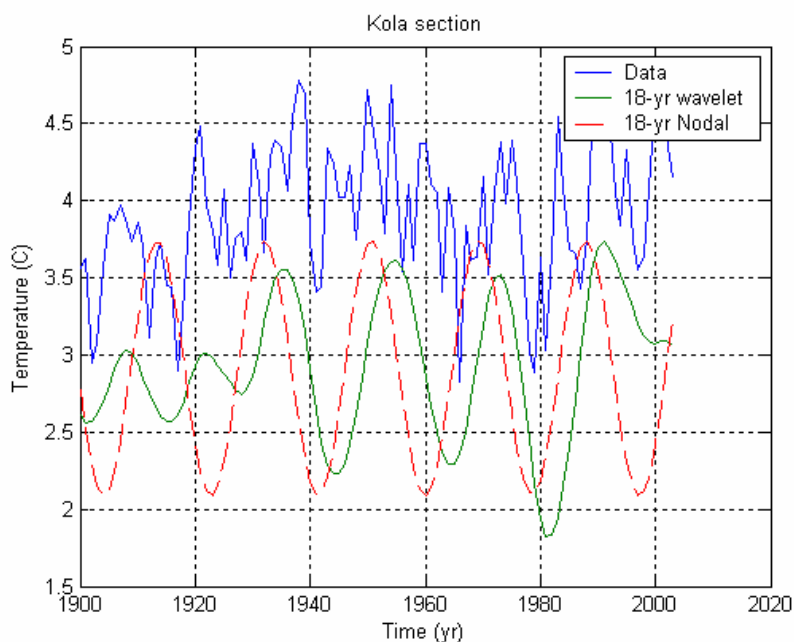


Figure 6 The Kola temperature time series, dominant 18 yr wavelet cycle and the 18.6 yr lunar nodal cycle.

Figure 6 shows the Kola section temperature time series and the dominant wavelet cycles of 18 and 55 years. The 55 yr cycle has a maximum at $W_{\text{KolTmp}}(55, nT)_{\text{max}} = \{1945, 2000\}$. The 18 year cycle has a maximum at $W_{\text{KolTmp}}(18, nT)_{\text{max}} = \{1909, 1922, 1935, 1955, 1973, 1991\}$. The dominant 18 yr wavelet cycle has a delay of $0.35 p$ (rad) or $18.6 * 0.35 / 2 = 3.2$ years compared to the 18.6 yr lunar nodal cycle. The cycle has p (rad) phase-reversal at about the year 1920. The cross-correlation to the 18.6 yr lunar nodal tide is estimated to $R_{\text{KolTmp}}(18) = E[W_{\text{KolTmp}}(18, nT)U_{\text{nod}}(18, nT)] = 0.82$ when the cycle was

reversed in the period $n= 1920$ to 2003. The signal to noise relation is estimated to $S/N=3.0$ when the signal is wavelets of 6, 18 and 55 years.

The Kola section salinity time series

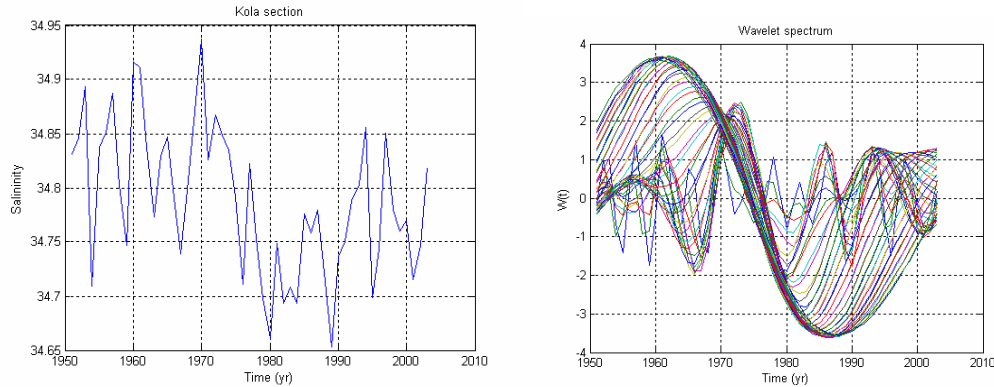


Figure 7 Time series of Kola section salinity and the computed wavelet spectrum.

Figure 7 shows the Kola section salinity time series and the computed wavelet spectrum. The wavelet spectrum $W_{\text{KolTmp}}(4:30, nT)$ has dominant cycles of about 6 and 18 years.

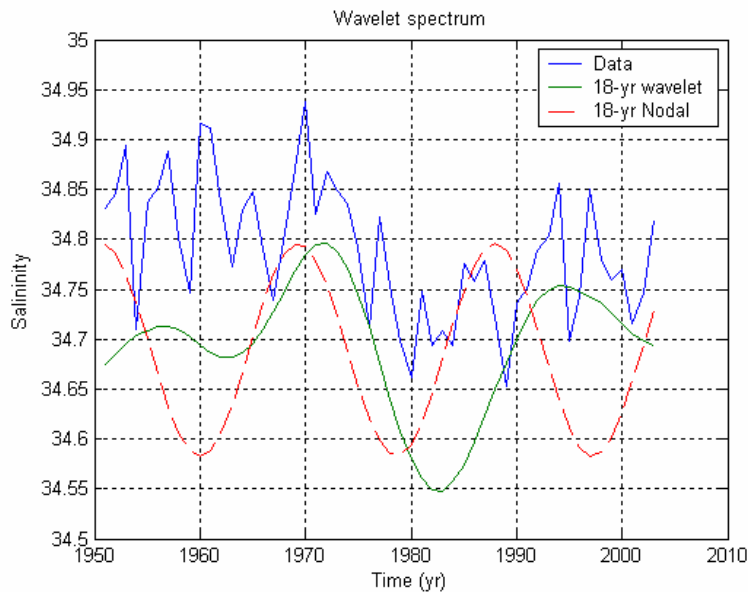


Figure 8 The Kola salinity time series, the dominant 18 yr cycle and the 18.6 yr lunar nodal cycle. The cycles are scaled on the presentation.

Figure 8 shows the data series and the dominant 18 yr cycle and the 18.6 yr lunar nodal cycle. The 18 yr wavelet cycles has a delay of about $0.35p$ (rad). This phase delay corresponds to the 18 yr Kola temperature cycle. The correlation to the lunar nodal cycles is estimated to $R_{\text{KolSal}}(18)=E[W_{\text{KolSal}}(18, nT, -0.35p)U_{\text{nod}}(18, nT)]=0.80$. The time series has a strong 6 year lunar nodal cycle. This cycle has a phase-reversal in 1978.

Summary

Time Series	Nodal spectrum ω_0 (rad/yr)	Cycle phase f (rad)	Phase reversals	Nodal cycle correlation R	Corr Quality Q	Signal Noise (S/N)
Atlantic						
$U_{AbTide}(18,nT)$	$\omega_0 nT$	(0.90-0.0)p		0.67	7.5	2.5
$U_{AbTide}(37,nT)$	$2\omega_0 nT$	1.40p		0.94	23.0	2.5
$U_{FarTmp}(18,nT)$	$\omega_0 nT$	(0.90-0.0)p	1920	-0.91	18.0	5.4
$U_{FarTmp}(55,nT)$	$\omega_0 nT/3$	(0.90-0.4)p		0.80	13.1	
$U_{FarSal}(18,nT)$	$\omega_0 nT$	(0.90+0.0)p	1920, 1980	0.82	8.7	2.6
$U_{FarSal}(55,nT)$	$\omega_0 nT/3$	(0.90-0.4)p		0.86	17.8	
$U_{ScoTmp}(18,nT)$	$\omega_0 nT$	(0.90+1.0)p	1920	0.86	14.2	4.8
$U_{ScoTmp}(55,nT)$	$\omega_0 nT/3$	(0.90+0.0)p	1920	0.92	24.0	4.8
$U_{ScoSal}(18,nT)$	$\omega_0 nT$	(0.55+0.0)p				2.6
$U_{ScoSal}(74,nT)$	$\omega_0 nT/3$	(0.90-0.0)p		0.91	25.5	2.6
Barents Sea						
$U_{HamTmean}(06,nT)$	$3\omega_0 nT$	(-0.09+0.15)p	1978	0.5	1.2	1.74
$U_{HamTmean}(18,nT)$	$\omega_0 nT$	(0.90-0.25)p		0.82	9.4	1.74
$U_{HamTmax}(18,nT)$	$\omega_0 nT$	(0.90-0.75)p		0.90	13.3	2.2
$U_{HamTmin}(18,nT)$	$\omega_0 nT$	(0.90-0.0)p		0.82	10.5	2.1
$U_{KolTmp}(06,nT)$	$3\omega_0 nT$	-1.09/-0.09p	1920, 1978			
$U_{KolTmp}(18,nT)$	$\omega_0 nT$	(0.90-0.35)p	1920	0.82	13.0	3.0
$U_{KolTmp}(55,nT)$	$\omega_0 nT/3$	(0.90-0.0)p		0.87	18.0	3.0
$U_{KolTmp}(74,nT)$	$\omega_0 nT/4$	(0.29-0.0)p		0.95	34.0	3.0
$U_{KolSal}(06,nT)$	$\omega_0 nT$	-1.09/-0.09p	1978			
$U_{KolSal}(18,nT)$	$\omega_0 nT$	(0.90-0.35)p		0.8	9.4	2.6

Table 1. Summary of the investigation ($p=3.14$).

Table 1 shows a summary of the time series investigations. U_{AbTide} represents the sea level time series at Aberdeen, U_{FarTmp} the temperature at Faroe side, U_{FarSal} the salinity at Faroe side, U_{ScoTmp} the temperature at Scottish side, U_{FarSal} the salinity at Scottish side, $U_{HamTmean}$ the mean sea level at Hammerfet, $U_{HamTmax}$ the maximum sea level at Hammerfest, $U_{HamTmin}$ the mean sea level at Hammerfest, U_{KolTmp} the Kola section temperature, U_{KolSal} the Kola section salinity. The high nodal cycle correlation and correlation quality Q shows there is a close relation between fluctuation in the time series and the 18.6 year lunar nodal tide. The high signal to noise relation S/N shows that the harmonics from the 18.6 yr tide has a dominant influence on the fluctuations in the time series.

The Northeast Atlantic:

The annual mean sea level at Aberdeen has dominant lunar nodal cycles of about 6, 18 and 37 years. The 18 year cycle $U_{AbTide}(18,nT)$ is closely related to the 18.6 year lunar nodal tide cycle.

The temperature time series of MNAW on the Faroe side of the Faroe-Shetland Channel has dominant lunar nodal cycles of about 6, 18 and 55 years. The 18 yr temperature cycle is closely correlated to the 18 yr sea level cycle at Aberdeen and 18.6 yr lunar nodal cycle (Pugh, 1996). This indicates that the dominant 18 yr temperature cycle is controlled by the 18.6 yr lunar nodal tide. The 18 yr cycle had a phase-reversal in about 1920. The phase-reversal introduces a time variant process controlled by an unknown source. The MNAW salinity time series has dominant cycles of about 6, 18 and 55 year. The 18 yr cycle has the same phase as the 18 yr temperature cycle. The time series had a phase-reversal in about 1920 and 1980.

The NAW temperature cycle, on the Scottish side of the Faroe-Shetland Channel, has dominant cycles of about 6, 18 and 55 years. In this time series the 18 yr cycle has a phase shift of $1.0p$ (rad) compared the 18 yr temperature cycle on the Faroe side and the 18.6 yr lunar nodal tide. In this time series there was a phase-reversal in about 1920. The NAW salinity time series has a dominant cycle of about 55 years. In this time series the 18 yr lunar nodal cycle was not identified.

The Barents Sea:

The annual sea level at Hammerfest has dominant lunar nodal cycles of about 6 and 18 years. The 18 year cycle $U_{\text{HamTide}}(18,nT)$ has a delay of $0.25p$ (rad) or 2.3 years compared to the 18.6 yr lunar tide cycle. The annual minimum sea level $U_{\text{HamTmin}}(18,nT)$ has a dominant 18 yr cycle which has the same phase as the lunar nodal tide. The annual maximum time $U_{\text{HamTmax}}(18,nT)$ series has a dominant 18 yr cycle which has a phase delay of $0.75p$ (rad) or 7.0 years compared to the 18.6 year lunar tide cycle.

The Kola section temperature data series has dominant lunar nodal cycles of about 6, 18, 55 and 74 years. The dominant 18 year temperature cycle has a delay of about of $0.10p$ (rad) or 1.0 year compared to the 18 year sea level cycle at Hammerfest. The Kola section salinity time series has dominant lunar nodal cycles of about 6 and 18 years. The dominant 18 yr cycle is close related to the 18 year Kola section temperature cycle.

Discussion

The materials and methods

The Faroe-Shetland Channel data series have some missing data the first 25 years. This influenced the identification of the 55 yr lunar cycle. The analysis was done by interpolating the missing data and by putting the missing data to zero. Both methods identified the 18.6 yr lunar nodal cycle.

The investigation identified dominant lunar nodal cycles of about 6, 18, 37, 55 and 74 years in the wavelet spectrum. The 6 yr cycle is difficult to identify in long periods. The cycle is influenced by noise and the 18 yr cycle seems to introduce phase-reversals on the 6 yr cycle. The best stationary cycle estimates are from the Barents Sea time series. Wavelet transforms have a surprising ability to identify long-term cycles. The problem is to reduce error at the ends of the time series. This error was reduced by the explained scaling method. The 55 yr and the 74 yr cycles are estimated in the short time series of about 100 to 110 years. These estimates should, however, be confirmed by analyzing more time series.

The best estimates are related to the identification of the dominant 18 yr cycles. The 18 yr cycle identification is confirmed by the sea level analysis and by astronomical data. The same cycles are identified by others (Maksimov and Smirnov, 1964,1965, 1967; Maksimov, and Sleptsov-Shevlevich, 1970; Yndestad, 1999, 2003). The coherence between the results from all time series confirms the good quality of the wavelet analysis method.

The lunar nodal spectrum

The investigation indicates that 18.6 year lunar nodal tide introduces a temporary 18 yr standing wave fluctuation in temperature and salinity. The fluctuation is observed in the time series from both the Faroe-Shetland Channel and the Barents Sea. The wavelet analysis has identified harmonic cycles of about 6, 37, 55 and 74 years. The source of these cycles is unclear and needs more investigation.

The relation between the Faroe-Shetland Channel and the Barents Sea time series

The investigation indicates that the fluctuations in the time series are controlled by the 18.6 yr lunar nodal tide. There is, however, a delay of about of 0.35p (rad) or 3.2 years between the 18 yr annual mean tide at Aberdeen and Hammerfest. This phase delay influences the fluctuating dynamics between the time series.

The identified stationary 18 yr cycles in the temperature and the salinity time series have stationary cycle times and long-term periodic phase-reversals. The cause of this phase-reversal is still unclear. In Arctic time series this phase-reversal is, however, associated with changes in sub-harmonic cycles (Yndestad, 2003). This indicates a modulation between the 18 yr cycle and sub-harmonic cycles. The phase-reversal may be caused by different processes in Faroe-Shetland Channel and in the Barents Sea. This property may introduce a new phase delay of 1.0p (rad) or 9.3 years between the 18 year cycle fluctuation in the Faroe-Shetland Channel and the Barents Sea.

Coherent or Chaotic regime shifts?

Chaotic regime shifts are associated with long-term cycles which are difficult to predict since they are dependent on the initial condition. In this analysis there are identified temporary stationary cycles from the lunar nodal tide which opens a new possibility of long term prediction. At the same time the phase-reversal property reduces the possibility of long-term prediction. The identification of the cause of the phase-reversal may be able to classify the regime shift properties. If the phase-reversals are caused by free oscillating systems, chaotic regime shifts would be expected. If it is caused by forced longer gravity from the moon, the regime shifts may be deterministic.

References

- Bochkov, Yu. A. 1982. Water temperature in the 0-200 m layer in the Kola-Meridian in the Barents Sea, 1900-1981. Sb. Nauchn. Trud. PINRO, Murmansk, 46: 113-122 (in Russian).
- Daubechies I. 1992. Ten lectures of wavelet. SIAM Journal on Mathematical Analysis. 24:499-519.
- Maksimov, I. V. and Smirnov, N. P. 1964. Long range forecasting of secular changes of the general ice formation of the Barents Sea by the harmonic component method. Murmansk Polar Sci. Res. Inst., Sea Fisheries, 4: 75-87.
- Maksimov, I. V. and Smirnov, N. P. 1965. A contribution to the study of causes of long-period variations in the activity of the Gulf Stream, Oceanology, 5, Pages 15-24.
- Maksimov, I. V. and Smirnov, N. P. 1967. A long-term circumpolar tide and its significance for the circulation of ocean and atmosphere. Oceanology 7: 173-178 (English edition).
- Maksimov, I. V. and Sleptsov-Shevlevich, B. A., 1970. Long-term changes in the tide-generation force of the moon and the iciness of the Arctic Seas. Proceedings of the N. M. Knipovich Polar Scientific-Research and Planning Institute of Marine Fisheries and Oceanography (PINRO), 27: 22-40.
- Matlab. 1997. Matlab. Wavelet Toolbox. Users Guide. The Math Works Inc.
- Pugh, D T. 1996. Tides, Surges and Mean Sea-Level. John Wiley & Sons. New York.

Yndestad, H: 1999a. Earth nutation influence on the temperature regime of the Barents Sea. ICES Journal of Marine Science. 56: 381-387.

Yndestad H: 2003a. A Lunar nodal spectrum in Arctic time series. ICES Annual Science Conference. Sept 2003. Tallinn. ICES CM 2003/T.